Gelation suppression in RAFT polymerization

Fang-Yi Lin, Mengguo Yan, and Eric W. Cochran*

Department of Chemical and Biological Engineering, Iowa State University, Ames, IA 50011

E-mail: ecochran@iastate.edu

Abstract

In this article we extend the understanding of gelation suppression in reversible addition-fragmentation chain transfer (RAFT) polymerization in systems with long primary chains and high crosslinker content, regimes which have been mostly overlooked to date. Using a model methacrylate system the gel point, apparent propagation rate constants and polymer architectures are seen to vary in a systematic fashion. By combining our experimental data with several related studies, we introduce a new phenomenological parameter, the "crosslinking tendency", that incorporates monomer concentration and excess functionality to universally describe the gelation suppression in both RAFT and ATRP controlled radical polymerization systems. The ability of the crosslinking tendency to quantitatively account for a broad range of RAFT and ATRP systems suggests that factors such as monomer architecture and details of activation/deactivation mechanisms may play only a secondary role in gel point suppression.

Keywords

Gelation, Crosslinking, Branched polymer, RAFT polymerization

Introduction

Branched and highly branched, often referred to as hyperbranched, polymers consist of a network of sub-chains stemming from the "primary chain." Multifunctional monomers, or "crosslinkers," cause branching; the gel point is the state in which branched chains interconnect to form an infinite network, at which point the polymers can neither be solvated nor processed thermally. With their networked architectures, branched polymers are useful in separations as membranes and chromatography materials.[1] Branched polymers also have wide applications as adhesives and additives due to the residual functionality that offers the capability of curing after application to enhance the mechanical strength.[2] To have enough mechanical strength for these type of applications, these polymers must have some minimal molecular weight. However, the introduction of crosslinker readily creates a situation in which the infinite network forms abruptly, making it difficult to design a polymerization that yields non-oligomeric yet finite branched polymers.

A better understanding of the branching process is therefore needed to elucidate the synthesis of branched polymers that meets industrial application criteria. The classical treatment considering infinite network formation was the gelation theory by Flory for step growth polymerization.[3] With the contemporary hypothesis of the rare instantaneously active radicals on a chain relative to other dormant groups, Stockmayer adapted this work to chain growth polymerization.[4] Two key assumptions are included in this theory: firstly, crosslinkers can only form bridges between *inter*molecular chains in a random manner; and secondly, different functional groups are equally reactive. The ideal infinite network is thus formed when there is only one branch point per chain. However, several studies have large deviations from Flory and Stockmayer (F-S) theory. For example, Matsumoto *et al.* showed that gel conversion, which is the vinyl conversion at the gel point, can be five times larger than the theoretical gel point in a free radical polymerization (FRP) system when there is a chain transfer agent.[5] This phenomenon, termed

gel-point suppression, has also been observed in FRP of styrenes and methacrylate systems.[6–9] Gel-point suppression is thought to be caused by the *intra*molecular crosslinking of chains during reaction, which adds cyclizations to the local chain architecture without contributing to the formation of the infinite network.[10] A major research effort in gelation studies aims to approach the theoretical prediction and provide appropriate explanations for the onset of suppression. Matsumoto suggested three possible causes of gelation suppression: a thermodynamic excluded volume effect of active radicals, a diffusion constraint of chains beyond a certain extent of reaction, and reduced reactivity of pendent groups, namely residual vinyl groups from crosslinker molecules that have already been incorporated into the chain.[5,9] These factors are not considered in F-S theory, and leads to the formation of a "microgel" in the early stages of polymerization, in which polymer chains crosslink and gel in a locally confined region. The microgel grows and eventually crosslinks with other microgels to reach the (macro)gel-point constituting a heterogeneous network constrained in expanse only by the reaction volume.[8,11]

Controlled radical copolymerizations (CRPs) have been considered as a potential way to approach ideal gelation conditions.[7,8] CRP reactions intentionally limit the radical concentration to suppress termination reactions and provide uniform chain initiation, yielding products with dispersity ($Đ$) nearing unity and molecular weight averages that are proportional to conversion. Atom-transfer radical polymerization (ATRP)[12–15] and reversible-addition fragmentation polymerization (RAFT)[16–19] are the most-practiced implementations of CRP. RAFT limits radical concentration through the introduction of chain transfer agents (CTAs) that readily form stable radical intermediates, whereas ATRP employs transition metal catalysts to reversibly activate and deactivate functional chain ends.[20] It is believed that in CRP processes, relatively homogeneous branched networks are formed due to the suppression of *intra*molecular crosslinking and the concomitant formation of microgels.[7,8,21,22] The suppression of microgel formation in CRPs, compared to FRP, is evidenced by the significant delay of the onset of Trommsdorff effect, which is

the autoaccelaration of polymerization as the diffusion of polymer chains is limited.[7]

The gelation process in CRPs has been discussed through several relevant reaction parameters. Many play some role in the kinetics and final network structures: solvent quality,[9] monomer concentration,[23] the amount of thermal initiator used (RAFT-specific),[24] temperature, the amount of crosslinker, the functionality of the crosslinker, the amount of CTA with respect to monomer and/or crosslinker (RAFT-specific) and the amount of the halide-initiator and catalyst/countercatalyst (ATRP-specific). Monomer concentration is perhaps the key factor throughout polymerization chemistry.[21,25] The critical "blob overlap" concentration in methacrylate systems has been shown to delineate *inter*molecular- vs. *intra*molecular-crosslinking-dominated behavior.[21] Additionally, the monomer concentration strongly influences the solution viscosity; in concentrated systems, diffusion-limited conditions develop in the late stages of polymerization, promoting network formation.[25] In RAFT polymerization, changing the ratio between the chain transfer agent and the monomer varies the target molecular weight.[26] With increasing CTA concentration the primary chain length will become shorter and the number of branch points per primary chains will decrease. The amount of crosslinker added is a vital factor in the formation of network structure. Controlling the ratio of CTA to crosslinker is a proven strategy to polymerize a high conversion product without gelation, although at cost of limited primary chain length. The "Strathclyde route" keeps the ratio of chain transfer agent to crosslinker around unity to prevent gelation.[25,27] The structure of the CTA also plays a role in the retardation of reaction rate.[26] Obviously, the crosslinker concentration controls the evolution of branching and ultimately crosslinking. While most of the literature keeps the crosslinker to monomer ratio quite small, there have been reports that increasing its value *increases* gel-point suppression with respect the F-S theory expectation.[5,28] This may be understood by considering that crosslinkers increase the tendency for both *inter*- and *intra*molecular linkages, the latter of which is not accounted for in the F-S treatment.

Beyond basic reaction parameters, the role of monomer architecture on gelation in CRPs is unclear. Tripathi *et al.*[29] indicated that longer alkyl ester side chains of monovinyl methacrylates significantly slow down the radical propagation through pendent vinyl groups in copolymerization with the crosslinker. Crosslinkers with bulky spacer groups are reported to promote *inter*molecular crosslinking during polymerization because of the steric hindrance.[30] Likewise, several reports indicate that shorter spacer groups promote *intra*molecular crosslinking.[31–33] However, Gao *et al.* found that the crosslinker architecture does not significantly influence gelation.[34] In our previous work, we reported that the polymerization of neat acrylated epoxidized soybean oil (AESO) by RAFT is strongly gelation-suppressed with as high as 85% monomer conversion achievable prior to macro-gelation.[24,35,36] These polymerizations of AESO are a departure from other CRP/crosslinker systems in a few key ways. Firstly, in contrast to most reports in which a small amount of di- or tri-functional crosslinker is added to a mono-functional monomer, AESO bears an average of 2.6 acrylic groups per molecule and was the sole polymerizable species. Secondly, AESO features a large molecular weight, approximately 1200 Da, comprising a bulky and flexible structure with over twenty spacer units separating acrylic groups. Finally, the gelation suppression effect persisted even when large primary chains (over 1 MDa) were considered. These results further questions regarding the role of crosslinker architecture; *e.g.*, is the bulky structure of AESO directly responsible for the large degree of gel-point suppression?

Therefore, it is interesting to consider gelation suppression in AESO in the context of several other studies treating this topic. With a considerable amount of literature focused on gelation behavior, however, some significant gaps have not yet been filled. Research to date has focused mainly in the dilute crosslinker regime such that the value of branches per chain is less than unity. With few exceptions,[13,25] the crosslinker to monovinyl monomer is less than 10%. However, gelation suppression is still expected at higher crosslinker levels as we have observed in the case of pure AESO polymerization. Moreover, in most

CRP gelation studies the degree of polymerization (DP) is typically less than 100. Nevertheless, (hyper)branched polymers will often require considerable molecular weight to be useful in applications, and thus there is a need to further investigate the polymerization of branched polymers with larger primary chain length. In this Article we address these gaps though the investigation of gelation suppression in RAFT polymerization on small-molecule methacrylate copolymers, in contrast to the bulky AESO monomers treated in our previous work, focusing on large primary chain size and crosslinker concentration.

Experimental

Materials

Methyl methacrylate (MMA) and ethylene glycol dimethacrylate (EGDMA) were purchased from Fisher and Sigma-Aldrich, respectively. Monomers were passed through an inhibitor remover column before conducting reactions. Azobisisobutyronitrile (AIBN) was purchased from Sigma-Aldrich and recrystallized by methanol. Cumyl dithiobenzoate (CDB), which serves as the chain transfer agent in RAFT polymerization, was used as supplied from Sigma-Aldrich. Phenothiazine and methyl ethyl ketone (MEK) were used as supplied from Aldrich and Fisher, respectively.

RAFT copolymerization of methyl methacrylate and ethylene glycol dimethacrylate

The detailed recipe for each copolymerization reaction is in Table 1. The prescribed amounts of MMA, EGDMA, AIBN, and CDB were mixed in the round-bottom flask and purged under argon. The MMA to CDB molar ratio was 998, and the AIBN to CDB ratio was 0.3. The reactions were carried out at 80 ^{o}C and stirred at 600 rpm. The kinetics were verified by taking aliquots to acquire the conversion and molecular weight during the

progression of the copolymerization. The gel point was determined as the time when the vortex generated by the stir bar vanished. Every entry showed in Table 1 was successfully replicated at least three times. Approximately 500 ppm phenothiazine was added into the aliquot solution to prevent further crosslinking. The products were crashed by methanol and vacuum dried.

Characterization

Conversions of polymerization were obtained from ^{1}H NMR spectra recorded in deuterated dimethyl sulfoxide (DMSO) with a Bruker Avance III spectrometer (600 MHz). The molecular weight distribution was characterized by an integrated gel permeation chromatography (GPC) system using chloroform as the eluent. Details of the integrated GPC system are as follows: a 515 HPLC pump and 717 autosampler were obtained from Waters with a chloroform flow rate of 1 ml/min. Three chromatography columns with the molecular weight distributed between 1,000 and 1,000,000 Da along with a guard column were purchased from Agilent. The system was equipped with a Malvern 270 dual detector, which contains a viscometer, light scattering detectors angled at 7^o and 90^o, and a refractive index detector from Wyatt. The system was calibrated by polystyrene triple detection standards obtained from Malvern. Samples were prepared at 5 mg/mL in chloroform and passed through a 0.45 μm PTFE filter. Aliquots were also redissolved in MEK at a concentration of 5 mg/mL for characterization by dynamic light scattering (DLS). The DLS measurements were carried out on a Malvern Zetasizer Nano ZS with a light scattering angle of 173^o. The filtered samples were equilibrated at 20 ^{o}C for 180 s prior to measurement. The size by intensity information was averaged from 5 measurements. Poly(methyl methacrylate) (PMMA) standards used for comparison in DLS experiments were purchased from Polymer Laboratories.

Results

Table 1 summarizes the molar ratio of EGDMA to MMA ([DM]/[M]) and the overall vinyl concentration ([=]) used for different entries. Samples are encoded as DMM$X0Y$, where X indexes the vinyl concentration and Y indexes the [DM]/[M] ratio. The highest [DM]/[M] is set to 0.5 to account for the influence of a high branching ability on the gelation of the system. The average gel time ($t_{exp,gel}$) of each entry is listed in Table 1. The gel time is shorter with an increase of [DM]/[M] at constant monomer concentration. This trend is expected since crosslink density increases as more crosslinkers are involved. When varying the vinyl group concentration at the same [DM]/[M], the gel time is shorter at elevated concentrations. For entries at 1.0 M (DMM20Y), gelation only happens in DMM203. In the most diluted condition of 0.5 M (DMM10Y), no gelation takes place in all three entries. This implies that there is insufficient blob overlap for macro-gelation to occur, and thus only *intra*molecular crosslinking occurs.

Table 1: The summary of DMM ratio, vinyl group concentration, kinetic data, yield and the estimated gel time for each entry.

Sample code	$[DM]/[M]$	[=] /M	$t_{exp,gel}$ /min[a]	$X_{M,gel}$ /%	$X_{DM,gel}$ /%	X_g^{FS} /%[d]	$1000k_M$ $/min^{-1}$[e]	$1000k_{DM1}$ $/min^{-1}$[e]	$1000k_{DM2}$ $/min^{-1}$[e]	Yield /% [b]	$t_{DLS,gel}$ /min[f]	$\frac{\lvert t_{exp,gel}-tDLS,gel\rvert}{t_{exp,gel}}$ /%
DMM101	0.02	0.5	> 1440	> 21[b]	–	16	0.4	–	–	40	–	–
DMM102	0.2	0.5	> 1440	> 23[b]	–	6	0.3	–	–	43	–	–
DMM103	0.5	0.5	> 1440	> 13[b]	–	5	–	–	–	59	–	–
DMM201	0.02	1.0	> 1440	> 24[b]	> 11[b]	16		0.7	0.9	–	42	–
DMM202	0.2	1.0	> 1440	> 15[b]	–	6	–	–	–	68	–	–
DMM203	0.5	1.0	154	–	–	5	–	–	–	–	136.4	11
DMM301	0.02	2.9	281	33[c]	22[c]	16	1.5	2.0	0.7	–	277.0	1
DMM302	0.2	2.9	81	8[c]	6[c]	6	1.2	1.8	0.7	–	79.4	1
DMM303	0.5	2.9	68	8[c]	5[c]	5	1.2	1.4	0.5	–	66.2	2
DMM401	0.02	4.8	131	31[c]	36[c]	16	2.8	7.1	1.9	–	136.0	4
DMM402	0.2	4.8	53	11[c]	10[c]	6	2.0	3.6	2.1	–	54.1	2
DMM403	0.5	4.8	40	6[c]	5[c]	5	1.7	2.6	0.6	–	40.3	4

a 1/10 of the initial amount of initiator was replenished every 8 hr to ensure sufficient active radicals in the system.
b The conversions and mass yields were recorded at 1440 min.
c Gel conversions of MMA and DM are extrapolated to the gel point from kinetic data.
d The theoretical gel point (X_g^{FS}) is calculated based on eq 7.
e The apparent rate constants are calculated only before the replenishment of initiator and based on equation 1 to 6 after fitting with ex
perimental data from ^{1}H NMR.
f The estimated gel time is derived from the extrapolation of inverse hydrodynamic radius versus time from dynamic light scattering.

To analyze the reaction kinetics, the vinyl conversion in both MMA and EGDMA are measured with ^{1}H NMR spectra. EGDMA and MMA monomers are structurally similar with overlapping signals in the vinyl region of the spectra. However, the composition of two monomers and vinyl conversion can be resolved through the methoxy signals of MMA and the methyleneoxy signals of EGDMA in higher concentration entries ($[=] > 1.0\ M$). Figure S1 in the supporting information demonstrates the accuracy of using these signals to discern between unreacted EGDMA and MMA. Methyleneoxy signals from EGDMA (δ 4.37) and methoxy signals from MMA (δ 3.70) are clear without any overlapping indication in Figure S1(a). The integration of these peaks quantitatively determines the DMM ratio, as validated by a series of EGDMA/MMA mixtures of known composition as shown in Figure S1(b). These signals were further used to determine the conversion of monomers. Figure S2 in the supporting information shows an exemplary ^{1}H NMR spectrum from a partially completed DMM polymerization aliquot. Though signals of vinylic hydrogen (δ 6.04, 5.69) and allylic hydrogen (δ 1.90) from EGDMA and MMA are overlapped in the spectrum, signals are distinguishable from unreacted and reacted methoxy/methyleneoxy for both EGDMA and MMA. The vinyl conversion of EGDMA and MMA are analyzed from methoxy/methyleneoxy signals at (δ 4.37, 4.17) and (δ 3.70, 3.57). Using peak deconvolution to account for any peak overlapping, the corresponding conversion of EGDMA and MMA can be obtained. The conversions of EGDMA and MMA at the gel point ($X_{M,gel}$ and $X_{DM,gel}$) are listed in Table 1. At very dilute vinyl concentration, especially in higher [DM]/[M] entries, the sensitivity and accuracy of ^{1}H NMR analysis became limited. Hence the conversions of some entries were not considered in this work. Instead, mass yields after 24 hrs reaction are reported in Table 1 for non-gelled entries to give a surrogate of the conversion. Though the kinetics are slow at $[=] = 0.5$ M owing to gelation suppression, the yield of DMM polymers is at least 40%.

The development of the branched architecture throughout the polymerization is first

interpreted through the molecular weight distribution as measured through GPC. Figure 1 shows the progression of the polystyrene-calibrated number-average molecular weight (M_n) and the normalized molecular weight distribution in DMM403 and DMM201. The macro-gelation event is preceded by a rapid increase in the rate of molecular weight growth in DMM403, and is accompanied by a corresponding broadening of the molecular weight distribution that becomes multimodal. In contrast, macrogelation is completely suppressed over 24 h in DMM201; here the molecular weight grows at a nearly constant rate and the molecular weight distribution remains monomodal and comparatively narrow.

To assist in the identification of which crosslinking mechanism dominates during polymerization, Figure 2 plots the polystyrene-calibrated molecular weight versus conversion, $M_n(X)$, for all entries. In an "ideal" RAFT polymerization comprised solely of monofunctional monomers, all chains grow pseudo-simultaneously such that the molecular weight is linear in conversion, $M_{n,RAFT} = M_0 \frac{[=]_0}{[CDB]} X$ where X refers to the overall vinyl conversion, M_0 the molar mass per vinyl unit, $[=]_0$ the initial vinyl concentration. In the presence of crosslinkers, $M_n(X)$ is no longer a linear function; a propagation step that results in a new *inter*molecular crosslink will disproportionately increase the molecular weight. In contrast, *intra*molecular crosslinking will impart no net change to the mass of the molecule while reducing its hydrodynamic volume due to the new conformational constraint.[24,35,36] For this reason, *intra*molecular crosslinking causes the $M_n(X)$ to adopt a concave-down shape and may even give the appearance of a molecular weight reduction if the contraction of the hydrodynamic volume outweighs other growth mechanisms. Accordingly, the monotonic and positive deviation from linearity evident in Figures 2(c,d) is indicative that *inter*molecular crosslinking outweighs *intra*molecular crosslinking at medium and large crosslinker concentration. On the other hand, Figure 2(b) shows that for low crosslinker concentration $M_n(X)$ is nearly constant for $X \in [0.1, 0.2]$, revealing that *intra*molecular crosslinking are far more dominant in this regime.

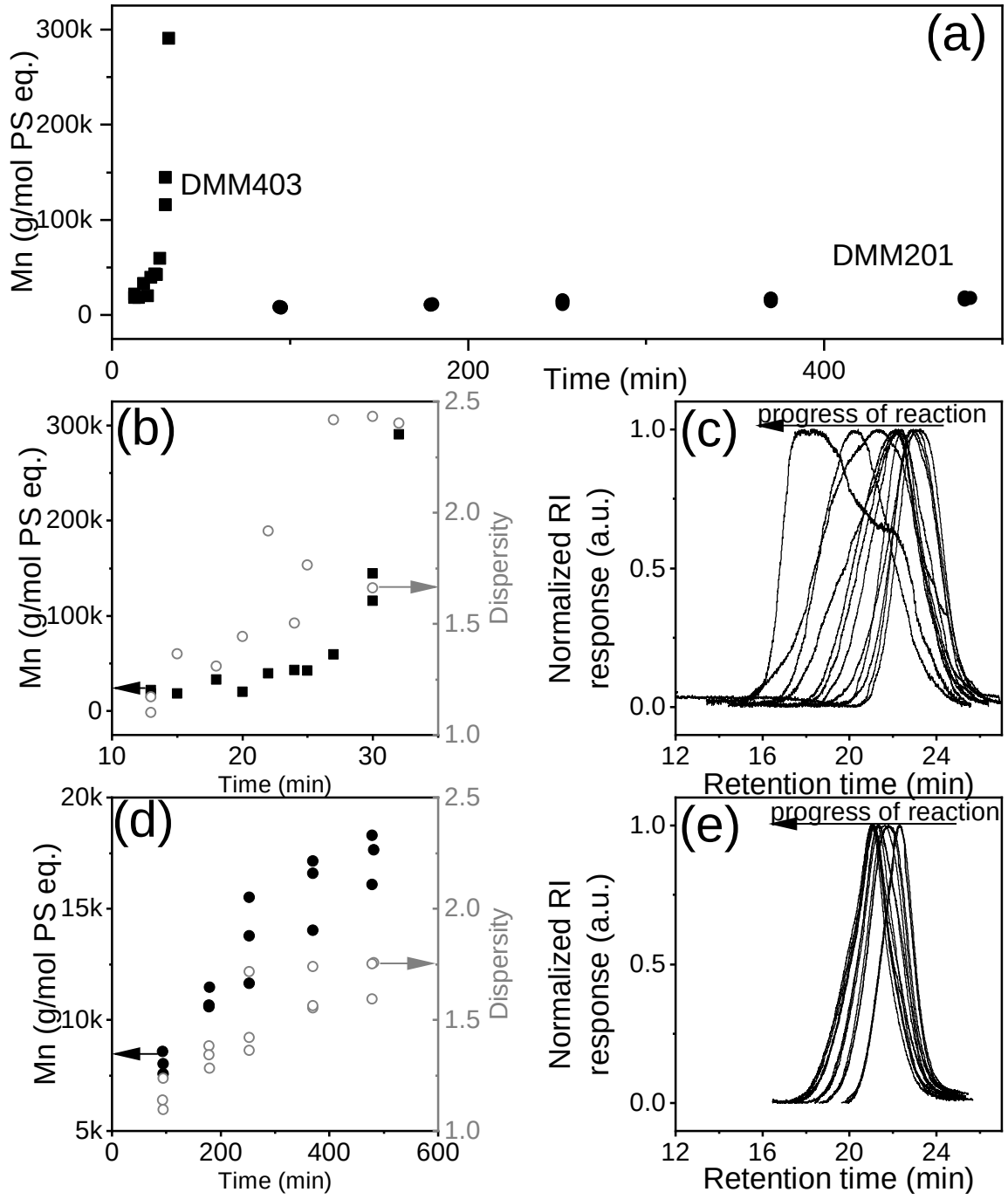

Figure 1: (a) The number-average molecular weight (M_n) of DMM403 (■) and DMM201 (●) with respect to time. The zoom-in M_n and dispersity (○) for (b) DMM403 and (d) DMM201. The corresponding RI response from GPC for (c) DMM403 and (e) DMM201 entries. The traces of RI response shown here were after peak height normalization.

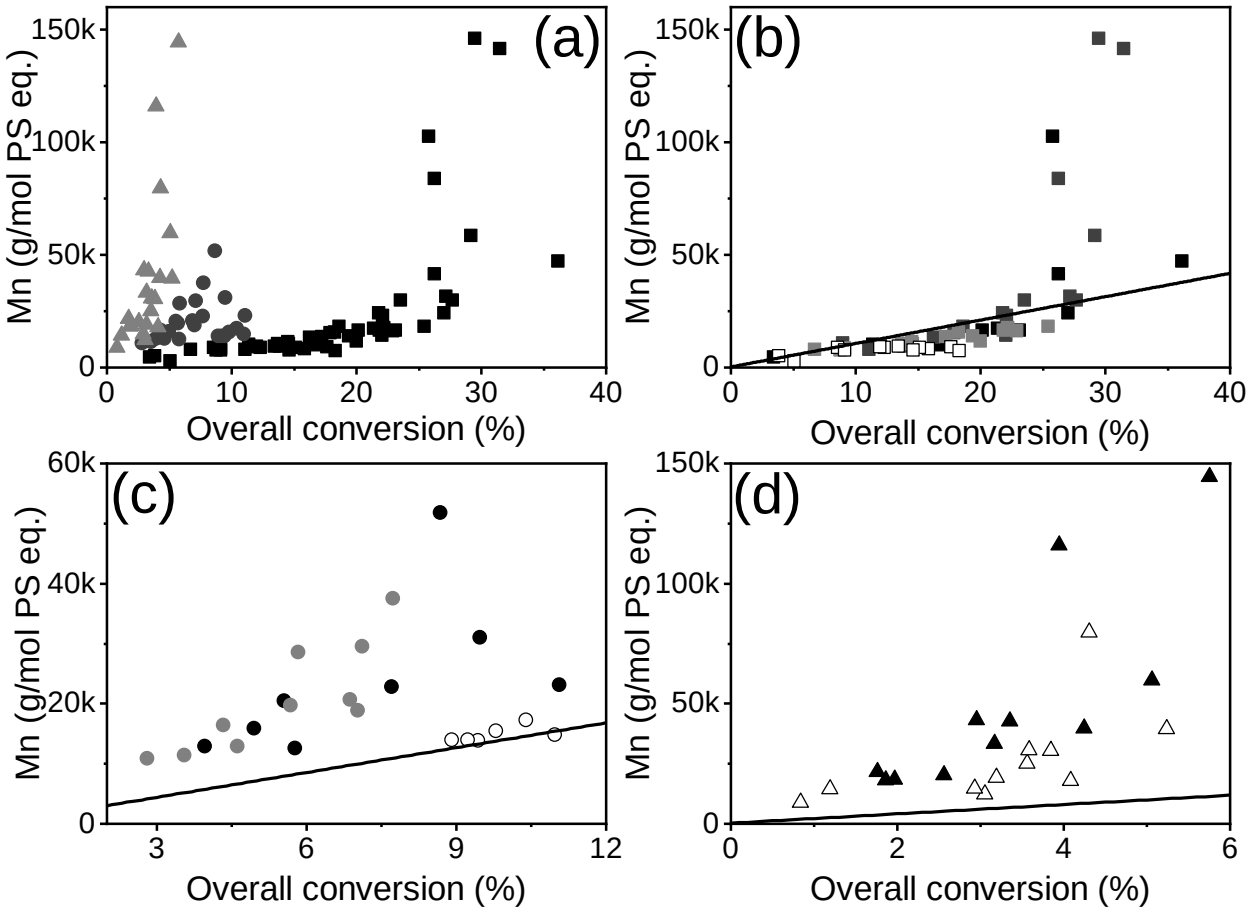

Figure 2: The number-average molecular weight (M_n) versus overall conversion at [DM]/[M] ratio of (a) all entries, (b) 0.02, (c) 0.2, and (d) 0.5. The straight lines indicate the theoretically linear manner of molecular weight versus overall conversion in RAFT polymerization assuming no branching occurred. Resulting from the low EGDMA conversion at 0.5 M vinyl concentration, the overall conversion in DMM101 and DMM102 trial only took MMA conversion into account. Symbols in (a) are ■ [DM]/[M] 0.02, ● [DM]/[M] 0.2, and ▲ [DM]/[M] 0.5. Symbols in (b)-(d) are ■ DMM401, ■ DMM301, ■ DMM201, □ DMM101; ● DMM402, ● DMM302, ○ DMM102; ▲ DMM403, and △ DMM303.

An important aspect of understanding the progression of crosslinking is the rate of crosslinking reactions compared to the rate of chain growth. Flory-Stockmayer theory treats all reactive sites as equally reactive, which is sensible based on the similar chemical environments. However, the steric environment of a vinyl group on a small monomer is quite different than that of a vinyl pendent group, and thus the apparent rate constant may be sensitive to these effects. The temporally resolved ^{1}H NMR spectra collected from

the aliquots in the various polymerization reactions described in Table 1 allows the consumption of vinyl in MMA to be distinguished from EGDMA. Therefore, we can obtain the kinetic information of each vinyl group in the propagation step by considering the concentration of different vinyl species, as shown in Scheme 1. The activity of the two vinyl groups in EGDMA is distinguished as follows: as a free molecule, the two vinyl groups in EGDMA are equivalent and thus have the same reactivity. However, once an EDGMA molecule joins a chain (reaction 2 of Scheme 1), the remaining vinyl group becomes pendent on the polymer chain (termed PDM) with a different steric environment. In reaction 3 of Scheme 1, this PDM group is consumed to form another branch point. The concentration of PDM is thus governed by the reaction of both vinyl groups. Since the propagation rate of each monomer is a first-order relationship with respect to monomer concentration, the consumption of the two vinyl groups on EGDMA can be identified independently. Therefore, apparent rate constants for each species can be extracted by least squares fits to these equations describing monomer consumption in these pseudo-living polymerizations. The depletion of each vinyl group from different monomers can be expressed as

$$\frac{d[M]}{dt} = -k_M[M] \tag{1}$$

$$\frac{d[DM]}{dt} = -k_{DM1}[DM] \tag{2}$$

$$\frac{d[PDM]}{dt} = k_{DM1}[DM] - k_{DM2}[PDM] \tag{3}$$

$$\frac{d[DDM]}{dt} = k_{DM2}[PDM] \tag{4}$$

where $[M]$ is MMA concentration, k_M is the apparent rate constant of MMA; $[DM]$ is EGDMA concentration, k_{DM1} is the apparent rate constant of the first vinyl group in EGDMA; $[PDM]$ is concentration of PDM, k_{DM2} is the apparent rate constant of PDM consumption, and $[DDM]$ is the concentration of $[DM]$ with fully consumed vinyl groups.

Thus k_M and k_{DM1} govern linear chain extension reactions whereas k_{DM2} the rate of branching or crosslinking. Though this process includes both *inter*molecular and *intra*molecular crosslinking, the magnitude of k_{DM2} with respect to k_{DM1} is a good indicator of the efficacy of the crosslinker.

The expression of vinyl conversions of MMA (X_M) and EGDMA (X_{DM}) through this model is therefore described as

$$X_M = 1 - \frac{[M]}{[M]_0} \tag{5}$$

$$X_{DM} = \frac{[PDM] + 2[DDM]}{2[DM]_0} \tag{6}$$

where C_{M0} and C_{DM0} are the initial concentration of MMA, and EGDMA, respectively.

Least squares fits of the data to the model yield k_M, k_{DM1}, and k_{DM2} values as tabulated in Table 1 and plotted in Figure 3 with $r^2 > 0.82$. Figure 3 shows that the apparent rate constants are higher under at higher monomer concentration. Under such conditions, i.e. [M] = 4.8 M, higher [DM]/[M] entries show lower apparent rate constants compared to low [DM]/[M] entries. k_{DM1} is comparable to or slightly larger than that for consumption of the analogous vinyl in MMA; k_{DM2} is consistently 20–50% of k_{DM1}, which strongly suggests that steric factors significantly influence the effective reactivity of the pendent vinyl groups.

The change in hydrodynamic radius (R_h) throughout the polymerization was characterized by DLS in MEK. The aliquot samples were redissolved in MEK at 5 mg/mL. The solution is considered in the dilute solution region since the overlap concentration of

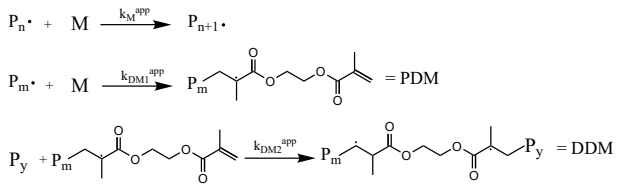

Scheme 1: Propagation steps for different monomer species in the reaction.

methacrylates is reported as ~ $10\ \%\ w/v$.[23] Due to the high $Đ$ values, the non-negatively constrained least-squares (NNLS) method was used to analyze the autocorrelation function, which assumes a broad monomodal or multimodal distribution of solutes.[37] Figure 4 shows exemplary R_h^{-1} versus the square root of time for gelled and non-gelled entries. It shows that R_h^{-1} is linearly related to time for the gelled entries. According to Flory, gelation is defined as the point when polymer constructs an infinite network such that $R_h \to \infty$. Therefore, theoretically when $t = t_{gel}, R_h^{-1} \to 0$. The extrapolated gel time by DLS ($t_{DLS,gel}$) and the deviation from the observed $t_{exp,DLS}$ are summarized in Table 1. $t_{DLS,gel}$ is close to $t_{exp,gel}$, which indicates that the size of polymer from DLS is able to predict the gel point and locates the stage of polymerization during the reaction. On the other hand, for non-gelled entries, R_h does not increase with time after some point in spite of reaction progress. The inverse R_h of the non-gelled entry therefore can be expressed as an exponential decay function in the absence of gelation after 24 hrs. This exponential decay expression clearly exhibits the suppression of gelation resulting from the lack of macrogel formation by *intra*molecular crosslinking.

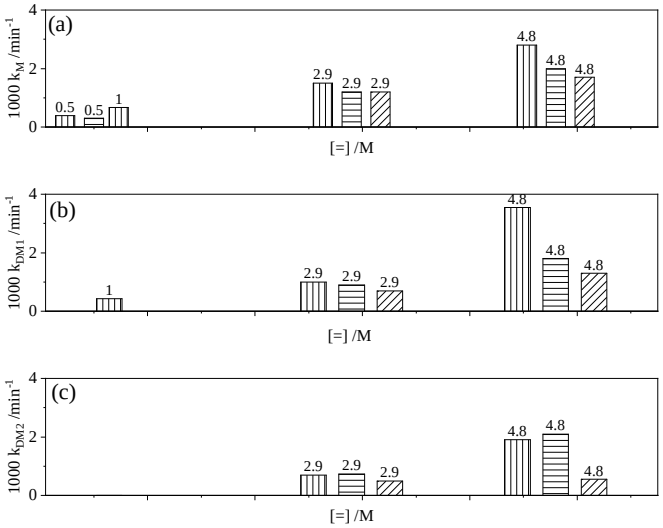

Figure 3: The calculated apparent rate constants of (a) MMA (k_M), (b) 1st vinyl group of EGDMA (k_{DM1}), and (c) 2nd vinyl group of EGDMA (k_{DM2}) at different reaction conditions. [DM]/[M] values of 0.02, 0.2, and 0.5 are illustrated as ◫, ⊟, and ◪, respectively.

Figure 5 depicts the relationship of R_h with respect to weight-average molecular weight (M_w). It is noted that R_h are merely grouped by [DM]/[M] but not vinyl concentration since we realized that R_h is insensitive to [DM]/[M] by linear regression. Figure S3 in the Supporting Information gives the example of R_h versus M_w of DMM203, DMM303, and DMM403 entries. The scaling exponents from the linear regression are roughly identical. Entries denoted in Figure 5(b) for different [DM]/[M] are from DMM201, DMM202, and DMM103. Due to the insufficient fitting of the autocorrelation function for particle sizes smaller than 10 nm, results from DMM101 and DMM102 are omitted. The size of polymers, either R_h or radius of gyration (R_g), is related to molecular weight to study the state of polymer in solution. In dilute solutions, polymers have the scaling behavior expressed as $R_g \sim R_h \sim M_w^{\alpha}$. The value of α is dependent on both solvent quality and polymer structure.[20] Table 2 summarizes the linear regression results of α and r^2 in Figure 5. The reference of linear PMMA standards shows α at 0.52 for this condition. In gelled entries, α decreases with increasing [DM]/[M]. In non-gelled entries, both [DM]/[M]= 0.02 and [DM]/[M] = 0.2 entries display smaller α than their gelled counterparts while α remains at 0.4 for [DM]/[M] = 0.5 entry.

Table 2: Summary of the scaling exponent (α) and the corresponding r^2 of different trials in Figure 5

	Gelled				Non-gelled		
$[DM]/[M]$	0	0.02	0.2	0.5	0.02	0.2	0.5
α	0.52	0.55	0.47	0.41	0.44	0.35	0.4
r^2	0.99	0.94	0.94	0.94	0.98	0.86	0.92

Discussion

We constructed a model system based on methacrylates to study gelation suppression in branched polymers with high targeted molecular weight and high crosslinker content. Clearly, both vinyl concentration and crosslinker content influence gelation. In this sec-

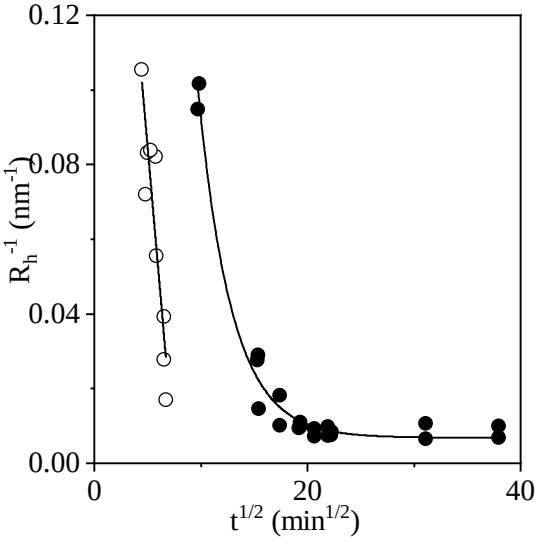

Figure 4: Inverse hydrodynamic radius (R_h^{-1}) versus inverse square root of time ($t^{-1/2}$) for a gelled entry (DMM402 ◯), and a non-gelled entry (DMM202 •.) The relationship is linear for the gelled entry while the inverse R_h exponentially decreased and leveled off in the non-gelled entry.

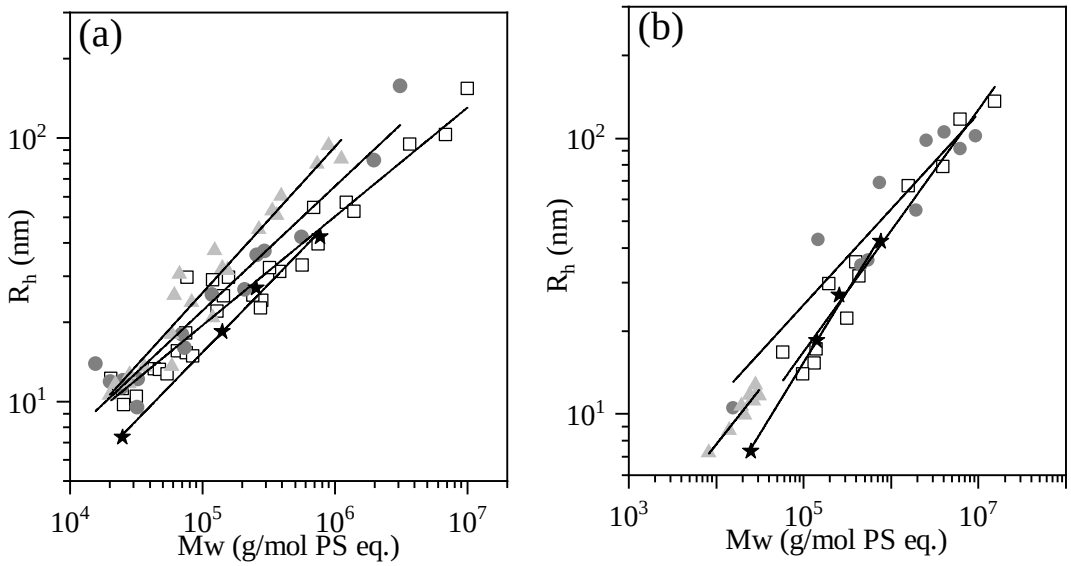

Figure 5: Hydrodynamic radius (R_h) of different DMM ratio versus weight-average molecular weight (Mw) for (a) gel, and (b) non-gelled trials. Symbols are □, •, ▲, and ⋆ for [DM]/[M] of 0.5, 0.2 ,0.02, and 0, which is linear PMMA, respectively.

tion, we discuss gelation suppression from a few different perspectives: first, the role of reaction kinetics on gelation is discussed from the observation of rate apparent constants. Second, the influence of crosslinker content on branched polymer structures and the subsequent solution behavior are discussed from the point of hydrodynamic radius. Third, gelation suppression is examined through the comparison of gel conversions between theoretical predictions and experiments. Our observations suggest the introduction of a new parameter, the *crosslinking tendency* (CT), a phenomenological parameter that incorporates monomer, crosslinker and reaction condition parameters. Finally, we show that the CT well-describes gelation suppression in several systems including those considered in this study as well as several other multifunctional RAFT and ATRP systems reported in the literature.

It is well-known that the termination step is diffusion-controlled in FRP due to the sluggish motion of large polymer chains. However, termination is strongly suppressed in CRPs and mass transfer effects on reaction kinetics are less obvious. However, this is not the case in crosslinker-contaminated CRP systems. The activation/deactivation of radicals, the key step in CRPs, becomes diffusion-controlled since the molecular weight increases dramatically from chain branching and network formation, especially at the later stages of polymerization.[7,38] This implies that diffusion limitation should become more severe at higher crosslinker content if other reaction parameters are kept constant. Indeed, the impact of mass transfer effects in our system is readily apparent through the pronounced reduction in the k_M and k_{DM1} rate constants as the crosslinker content increases (*cf.* Table 1 and Figure 3). A similar effect was reported by Bannister *et al.*,[39] in which crosslinker-containing polymerizations required up to six times longer to reach the same conversion compared an analogous monofunctional polymerization. The observation of viscosity change is another probe to observe the polymerization. Visual observation confirmed that the viscosity changes dramatically at near-gelation stage in concentrated entries. Since the reactions were agitated through magnetic stirring rather

than a mechanically driven impeller, mass transfer limitations should be particularly important in the late stages of polymerization. We suspect that fluid dynamics play an important role with this regard. It would be worthwhile to investigate on the impact of stirring/viscosity on reaction kinetics and the subsequent product structures in the future.

Flory-Stockmayer theory assumes equal reactivity for all vinyl groups; the results in Figure 3 show that this assumption is clearly violated for the EGMDA/MMA system in a manner consistent with the gel-point suppression effect. The values of k_M and k_{DM1} are comparable in most entries, which implies that the reactivity of MMA and the first vinyl group of EGDMA is similar as would be anticipated based on the chemical similarity. The reactivity ratio of MMA and EGDMA in free radical polymerization is reported as 0.67 and 1.49, which indicates that the copolymerization of MMA and EGDMA yields nearly random copolymers.[40] While our results of k_M and k_{DM1} support the formation of nearly random copolymers, the values of k_{DM2}, which reflect the rate constant for branch formation, is consistently only 20–50% of the corresponding k_{DM1} value. Once EGMDA has been incorporated into a growing chain, its second vinyl moiety remains available to act as a branch point in a subsequent reaction. Compared to the k_{DM1} value, the reactivity of the pendent vinyl group is reduced, which may be accounted for by both kinetic and thermodynamic considerations. From a kinetically-oriented perspective, the reaction of the first vinyl group requires the impingement of an active polymer radical with a small molecule; this diffusive process should be expected to occur more quickly than the impingement of an active polymer radical with a polymer pendent group. Thus the reactivity of pendent vinyl groups is relatively lower due to mass transfer effects. From a thermodynamic perspective, the "excluded volume effect" describes the fact that there are fewer conformationally accessible sites on pendent vinyl groups compared to free molecules.[41] Accordingly, the unequal reactivity of vinyl groups in EGDMA violates the ideal assumptions posed by Flory-Stockmayer theory and contributes to gel point sup-

pression.

Together with the reaction kinetics, the abundance of difunctional monomers controls the stochastic process of chain branching, which in turn determines the conformational character of the system. One manner in which this is expressed is through the dependence of R_h on M_w. This dependence is strongly affected by the [DM]/[M] ratio, reflecting the influence of this parameter on chain architecture, primarily branch length, or the average chain length between two adjacent branch points. Since the targeted DP is fixed for all entries, entries with lower [DM]/[M] values have fewer branch points and thus longer branch length. Polymer chains with longer branch length are more flexible and approach linearity as the crosslinker species is eliminated. For example, at [DM]/[M] = 0.02, α = 0.55, indicative of flexible chains similar in character to perfectly linear PMMA. The impact of branch length on the scaling behavior was recently demonstrated by Schmidt *et al.* by multiscale simulation.[42] In their work, four monomers with varied Kuhn lengths are used to calculate polymer properties as a function of molecular weight using atomistic Langevin calculations with a coarse-grained bead-and-spring model. They predict that polymers with shorter branches have a smaller α value (more globular) in agreement with our findings. The scaling behavior is also linked to the conformational state of polymers in solution. In flexible polymers, α equals 0.5–0.6 for freely swollen branched clusters in good solvent and decreases to 0.4 for poorly swollen branched clusters with fractal structure.[43] This phenomenon can also be seen in our study: comparing gelled and non-gelled entries at fixed [DM]/[M] for [DM]/[M] = 0.02 and 0.2, non-gelled entries show a smaller α-value than their gelled counterparts. Resulting from *intra*molecular crosslinking, chains are constrained more in non-gelled entries because of the formation of microgel. The heterogeneity of structures leads to reduced swelling as indicated by the decrease of α from gelled to non-gelled pairs. For [DM]/[M] = 0.5, α-values for gelled and non-gelled entries are similar, which may be explained by the more severe degree of branching present at all stages of polymerization in this system. DMM103 did not gel

because of the low vinyl concentration. Moreover, several simulation studies have shown that for hyperbranched polymers, the sphere-like conformation gives rise to similar features as of dendrimers, which is revealed by the scaling behavior of $\alpha \approx 0.33$.[44,45] The α of 0.35 in DMM202 is consistent with that of dendrimers, which indicates that polymer chains form a dendritic-like structure in this condition.

The crosslinking mechanism is most closely connected to the vinyl concentration. Studies have shown that when crosslinker-to-monovinyl monomer ratio of methacrylates is below 0.1, the critical overlap concentration of MMA gelation suppression is 10 wt% , which corresponds to vinyl concentration of 1.0 M in RAFT polymerization.[21,23] This phenomenon is consistent with our finding of DMM 201, and even DMM202. The crosslinking effectiveness is improved when more crosslinkers are involved, therefore the system gels in DMM203, which has the highest [DM]/[M].

According to Flory-Stockmayer (F-S) theory, the gel conversion is predicted as[4,5,24]

$$X_{gel}^{FS} = \left(\frac{x[C]_0 Đ}{[PC]_t} \right)^{-0.5} \tag{7}$$

where x is the functionality of crosslinker, $[C]_0$ is the initial crosslinker concentration, $Đ$ is the primary chain dispersity at time t, and $[PC]_t$ is the concentration of primary chains at time t which theoretically equals the concentration of chain transfer agent in RAFT or initiator species in ATRP. Since the ratio between primary chain concentration and the crosslinker concentration is fixed for the same [DM]/[M], in the present work the F-S gel conversion is fixed irrespective of vinyl concentration. The F-S gel conversions are listed in Table 1 assuming primary chains are monodisperse, and thus slightly overestimate the F-S gel point conversion.

The degree of gel-point suppression is evident in comparison of the experimental and F-S values. The two-fold increase in gel-point conversions of [DM]/[M] = 0.02 compared to the F-S values can be largely attributed to *intra*molecular crosslinking, which consumes

surplus vinyl groups with no contribution to the formation of the infinite network. In contrast to previous crosslinking studies that explore comparatively low crosslinker content and primary chain length, the high crosslinker contents and high target DP in the present study far more strongly favors *inter*molecular crosslink formation. To facilitate the comparison of several data sets spanning a broad range of reaction parameters, we introduce a simple phenomenological parameter, the "crosslinking tendency" (CT). The CT value may be simply viewed as the ratio of the concentration of excess vinyl content to the number of primary chains per crosslinker:

$$CT = [M_{tot}]_0(x-1)\frac{[C]_0}{[PC]_e} \tag{8}$$

Where $[M_{tot}]_0$ is the initial concentration of monovinyl monomer plus crosslinker, and $[PC]_e$ is the concentration of effective primary chains. The multiplication of first two terms describes the concentration of pendent vinyl crosslinkers. The last term is inherited from Flory-Stockmayer gelation theory, which posits that gelation occurs when each effective primary chain bears a crosslinker. In controlled radical polymerization, $[PC]_e$ depends on the concentration of CTA of RAFT or initiator of ATRP with a correction factor (η) to describe the efficiency of CTA or initiator. η is defined as

$$\eta = \frac{MW_{theo}}{MW_{exp}} \tag{9}$$

where MW_{theo} and MW_{exp} are the theoretical and experimental molecular weight of linear polymers, respectively. The concept of the efficiency of radical activation/deactivation was introduced by Matyjaszewski's group[46,47] in ATRP as the initiation efficiency, which is extended to RAFT here. The value of η is taken from the literature with the closest

reaction condition and reagents to our best attempt. $[PC]_e$ is then defined as

$$[PC]_e = \begin{cases} [CTA]\eta, & \text{in RAFT} \\ [I]\eta, & \text{in ATRP} \end{cases} \tag{10}$$

where $[CTA]$ is the concentration of CTA in RAFT; and $[I]$ is the concentration of initiator in ATRP. The values involved in the calculation of CT are included in the Supporting Information.

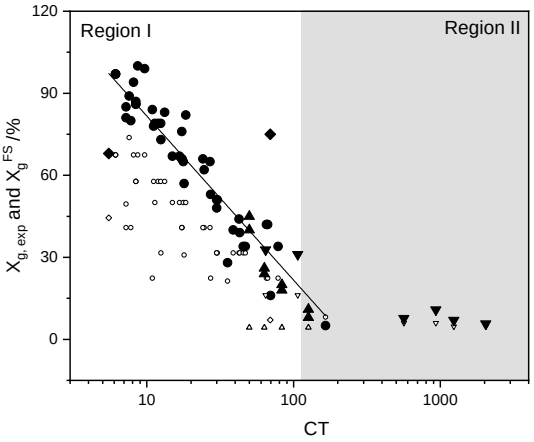

Figure 6: Experimental gel conversions $X_{g,exp}$ (filled symbols) and Flory-Stockmeyer predicted gel conversions X_g^{FS} (opened symbols) versus crosslinking tendency for this work (▼, ▽), our previous work of poly(acrylated epoxidized soybean oil) (▲, △), other RAFT (◆, ◇) and ATRP (●, ○) in the literature.[24,46–56] X_g^{FS} is calculated based on equation 7. The experimental gel conversions in region I is related to CT by $X_{g,exp} = 141.65 - 60log(CT)$ with $r^2 = 0.85$.

Figure 6 displays the gel conversions from experiments ($X_{g,exp}$) and F-S theory (X_g^{FS}) versus CT for both ATRP and RAFT systems from literature and the present study, which is labeled as ▼. The data reflect several different choices of chain transfer agent and ATRP catalyst/initiator formulations. Data points in Figure 6 are grouped into two regions based on the difference between gel conversions from F-S prediction and experiments. The boundary is placed at 10% gel conversion difference where CT ≈ 120. DMM301 and DMM401 feature low crosslinker content and high targeted DP, and thus lie in the low-CT

region (region I). These entries have similar gelation behavior compared to most of those from the literature. Gelation is severely suppressed in region I due to *intra*molecular crosslinking. Other data points from this study lie in high CT region (region II), which may explain why gel-point suppression is significantly reduced. The gelation behavior of RAFT in region II is seldom reported. The *inter*molecular crosslinking dominates in region II with high CT and leads to the more ideal network. It seems that the gel conversion is less sensitive to CT in region II compared to region I. This finding implies that the gelation suppression is highly related to the vinyl concentration of the system, which was not accounted for by F-S theory.

The strong linear correlation of $X_{g,exp}$ vs. $\log CT$ in region I using data from several RAFT and ATRP studies is very suggestive that CT accounts for the most significant parameters controlling the gel point. The data surveyed represent two very different CRP mechanisms, varied monomer/crosslinkers, ATRP catalyst/initiator formulations and RAFT chain transfer agents. Surprisingly, the ATRP entries in Figure 6 are indistinguishable from RAFT entries in region I where *intra*molecular crosslinking dominates. This observation implies that the starkly different nature of RAFT vs. ATRP does not play a significant role in the gel-point suppression phenomenon. In connection with our previous work, relating to poly(acrylated epoxidized soybean oil) (PAESO) synthesized by RAFT,[24] we found that gel-point suppression was most pronounced at low vinyl concentration. An unusual aspect with respect to gel-point suppression in this system is that it is comprised solely of crosslinker species with $x = 2.6$. The entries from this work are summarized in Figure 6 as ▲. Our original hypothesis was that the unique monomer structure of AESO strongly promoted *intra*molecular crosslinking during polymerization because of the large flexible AESO arms as compared to systems with smaller and more rigid molecules. To test this hypothesis, the entries of the present study feature smaller molecules and large crosslinker concentration. Interestingly, viewed through the perspective of CT-analysis, the PAESO system evidently resides in region I where CT strongly cor-

relates to the gel-point suppression and superimposes with several other small-molecule monomer systems. Because CT does not directly account for crosslinker size or other structural characteristics, we can conclude that gel-point suppression in the PAESO system is actually quite similar to other monomer systems. The bulky structure of AESO can be accounted for simply through its dilution of the total vinyl concentration. That is, the spacer groups behave like additional solvent in the system. As mentioned before, it is controversial how or whether the monomer structures affect gelation suppression. Our findings suggest that the spacer groups do affect the gelation behavior by means of diluting the vinyl concentration but not necessarily due to any special conformational effect.

The introduction of CT-analysis should thus be useful as a tool to predict the gelation behavior in RAFT and ATRP systems. By calculating CT values, whether the gelation of a system will be suppressed is predictable. For example the Strathclyde route, a method to prepare soluble branched copolymers, sets the crosslinker to primary chain ratio near unity. Based on the reaction conditions reported by Rosselgong *et al.*[57] in both RAFT and ATRP systems, the CT values of the branched methacrylate copolymers and the corresponding gel conversions predicted by CT (X_g^{CT}) are calculated and appear in Table S5 in the supporting information. The CT values of their results lie in between 1 and 6, which are in the gelation suppression region. According to the linear regression of CT in region I, the calculated X_g^{CT} values are between 98 and 142 %. If the prediction of CT-analysis is correct, in reality entries of predicted X_g^{CT} higher than 100% would not gel while entries of X_g^{CT} lower than or equal to 100% would gel. The CT-analysis thus predicts the gelation behavior of 20 out of 22 entries in their system. This example shows that CT is capable of predicting the gelation behavior. CT-analysis will become more robust if the information of more systems and more controlled radical polymerization methods is introduced in the future. There are several sources of error that may hinder the ability of CT-analysis to predict a gel-point conversion. Firstly, the manner in which the gel point

is reported varies somewhat among the various published studies. Secondly, the value of the efficiency factor η is difficult to measure directly in multifunctional systems and must be estimated based on analogous monofunctional systems. Thirdly, CT discounts other parameters that may significantly affect the gelation behavior such as the mass transfer properties and so on. Nonetheless, CT-analysis does present a simple manner in which several data sets spanning a broad range of reaction conditions collapse to a single "universal curve" with semi-quantitative predictive value for gel-point suppression.

Conclusion

Branched copolymer systems composed of MMA and EGDMA were constructed and polymerized by RAFT to study gel-point suppression, with particular attention to systems featuring high crosslinker content and long target primary chain length. The polymerization kinetics, polymer conformational data and gel-point information were measured as a function of vinyl concentration and crosslinker-to-monovinyl monomer ratio. A simple kinetic model was used to distinguish the apparent rate constants from different vinyl groups in the system. The difference of apparent rate constants implies the unequal reactivity of vinyl groups. The comparatively lower value of apparent rate constant from pendant vinyl group of the crosslinker is a consequence of both dynamic and thermodynamic considerations. The hydrodynamic radius of the polymers was used to identify the current stage of polymerization, determine if the polymerization should gel, and predict the gelation time. The scaling behavior correlated from M_w and R_h reveals the swellability and conformation information. Polymer chains with longer branch length show a better swellability, whereas non-gelled entries generally show reduced swellability and fractal- or even dendrimer-like structures.

The gelation mechanism is highly related to vinyl concentration governed by overlap concentration, which is about 1 M in our system. The crosslinking mechanism below 1 M

is dominated by *intra*molecular crosslinking; whereas the presence of *inter*molecular and *intra*molecular crosslinking above 1.0 M cause the gelation suppression. As *inter*molecular crosslinking becomes more important, shorter gel times and lower conversions at gel point are observed, corresponding to high [DM]/[M] entries, especially in concentrated conditions. A more homogeneous network is formed with higher [DM]/[M] where *inter*molecular crosslinking dominates. The transition between the intra- and inter-molecular crosslinking regimes appears to be well-described by a phenomenological parameter we refer to as the "crosslinking tendency", CT, which evidently accounts for the gelation behavior in both RAFT and ATRP systems. A system with high CT-value is dominated by *inter*molecular crosslinking, whereas a low-CT system is dominated by *intra*molecular crosslinking. This work and our previous gelation study in the PAESO system extends the investigation on gelation behavior in crosslinker-rich controlled radical polymerizations. The large spacer groups in AESO contribute to gel-point suppression by diluting the vinyl concentration. CT-analysis appears to semi-quantitatively predict the gel-point conversion through an empirical correlation although further confirmation is required. Overall, the kinetic data and the structural information presented herein reinforce the understanding of gelation mechanism in systems of high degree of polymerization and higher crosslinker content and can be useful in the design of hyperbranched materials where controlling the gel-point is desired.

Acknowledgement

The authors thank the support by United States Department of Agriculture (USDA-NIFA-CAM 2014-38202-22318) and United Soybean Board (USB 1740-362-0710).

Supporting Information Available

^{1}H NMR spectra, conversion calculation, R_h against M_w of [DM]/[M] 0.5 entries, numbers used in Figure 6 and numbers used in validating CT analysis.

This material is available free of charge via the Internet at `http://pubs.acs.org/`.

References

(1) Seiler, M. Hyperbranched polymers: Phase behavior and new applications in the field of chemical engineering. *Fluid Phase Equilibria* **2006**, *241*, 155–174.

(2) Czech, Z. Crosslinking of pressure sensitive adhesive based on water-borne acrylate. *Polymer International* **2003**, *52*, 347–357.

(3) Flory, J. Molecular Size Distribution in Three Dimensional Polymers. I. Gelation. *Journal of the American Chemical Society* **1941**, *63*, 3083–3090.

(4) Stockmayer, W. H. Theory of Molecular Size Distribution and Gel Formation in Branched Polymers II. General Cross Linking. *The Journal of Chemical Physics* **1944**, *12*, 125–131.

(5) Matsumoto, A.; Kitaguchi, Y.; Sonoda, O. Approach to Ideal Network Formation Governed by Flory-Stockmayer Gelation Theory in Free-Radical Cross-Linking Copolymerization of Styrene with m-Divinylbenzene. *Macromolecules* **1999**, *32*, 8336–8339.

(6) Scherf, R.; Müller, L. S.; Grosch, D.; Hübner, E. G.; Oppermann, W. Investigation on the homogeneity of PMMA gels synthesized via RAFT polymerization. *Polymer* **2015**, *58*, 36–42.

(7) Yu, Q.; Xu, S.; Zhang, H.; Ding, Y.; Zhu, S. Comparison of reaction kinetics and gelation behaviors in atom transfer, reversible addition-fragmentation chain trans-

fer and conventional free radical copolymerization of oligo(ethylene glycol) methyl ether methacrylate and oligo(ethylene glycol) dimetha. *Polymer* **2009**, *50*, 3488–3494.

(8) Norisuye, T.; Morinaga, T.; Tran-Cong-Miyata, Q.; Goto, A.; Fukuda, T.; Shibayama, M. Comparison of the gelation dynamics for polystyrenes prepared by conventional and living radical polymerizations: A time-resolved dynamic light scattering study. *Polymer* **2005**, *46*, 1982–1994.

(9) Matsumoto, A.; Okamoto, A.; Okuno, S.; Aota, H. Ideal crosslinked-polymers and their characterization in free-radical monovinyl-divinyl copolymerizations. *Angewandte Makromolekulare Chemie* **1996**, *240*, 275–284.

(10) Rosselgong, J.; Armes, S. P. Extent of intramolecular cyclization in RAFT-synthesized methacrylic branched copolymers using 13C NMR spectroscopy. *Polymer Chemistry* **2015**, *6*, 1143–1149.

(11) Davankov, V. A.; Tsyurupa, M. P. Structure and properties of hypercrosslinked polystyrene-the first representative of a new class of polymer networks. *Reactive Polymers* **1990**, *13*, 27–42.

(12) Kanamori, K.; Hasegawa, J.; Nakanishi, K.; Hanada, T. Facile Synthesis of Macroporous Cross-Linked Methacrylate Gels by Atom Transfer Radical Polymerization. *Polymer* **2008**, *41*, 7186–7193.

(13) Bouhier, M.-H.; Cormack, P. A. G.; Graham, S.; Sherrington, D. C. Synthesis of densely branched poly(methyl methacrylate)s via ATR copolymerization of methyl methacrylate and ethylene glycol dimethacrylate. *Journal of Polymer Science Part A: Polymer Chemistry* **2007**, *45*, 2375–2386.

(14) Gonçalves, M. A. D.; Dias, R. C. S.; Costa, M. R. P. F. N. Prediction and Experimental Characterization of the Molecular Architecture of FRP and ATRP Synthesized Polyacrylate Networks. *Macromolecular Symposia* **2010**, *289*, 1–17.

(15) Ali, M. M.; Stover, H. D. H. Well-Defined Amphiphilic Thermosensitive Copolymers Based on Poly(ethylene glycol monomethacrylate) and Methyl Methacrylate Prepared by Atom Transfer Radical Polymerization. *Macromolecules* **2004**, *37*, 8812.

(16) Jaramillo-Soto, G.; Vivaldo-Lima, E. RAFT copolymerization of styrene/divinylbenzene in supercritical carbon dioxide. *Australian Journal of Chemistry* **2012**, *65*, 1177–1185.

(17) Barlow (née Tan), K. J.; Hao, X.; Hughes, T. C.; Hutt, O. E.; Polyzos, A.; Turner, K. a.; Moad, G. Porous, functional, poly(styrene-co-divinylbenzene) monoliths by RAFT polymerization. *Polymer Chemistry* **2014**, *5*, 722–732.

(18) Leung, D.; Bowman, C. N. Reducing shrinkage stress of dimethacrylate networks by reversible addition-fragmentation chain transfer. *Macromolecular Chemistry and Physics* **2012**, *213*, 198–204.

(19) Moad, G. RAFT (Reversible addition-fragmentation chain transfer) crosslinking (co)polymerization of multi-olefinic monomers to form polymer networks. *Polymer International* **2015**, *64*, 15–24.

(20) Hiemenz, P. C.; Lodge, T. *Polymer chemistry*; CRC Press, 2007; p 587.

(21) Rosselgong, J.; Armes, S. P.; Barton, W.; Price, D. Synthesis of highly branched methacrylic copolymers: Observation of near-ideal behavior using RAFT polymerization. *Macromolecules* **2009**, *42*, 5919–5924.

(22) Poly, J.; Wilson, D. J.; Destarac, M.; Taton, D. A Comprehensive Investigation into "Controlled/Living" Chain Growth Crosslinking Copolymerization Including a Back to Basics Modeling. *Journal of Polymer Science Part A: Polymer Chemistry* **2009**, *47*, 5313–5327.

(23) Li, Y.; Ryan, A. J.; Armes, S. P. Synthesis of well-defined branched copolymers by quaternization of near-monodisperse homopolymers. *Macromolecules* **2008**, *41*, 5577–5581.

(24) Yan, M.; Huang, Y.; Lu, M.; Lin, F.-Y.; Hernández, N. B.; Cochran, E. W. Gel Point Suppression in RAFT Polymerization of Pure Acrylic Cross-Linker Derived from Soybean Oil. *Biomacromolecules* **2016**, *17*, 2701–2709.

(25) Isaure, F.; Cormack, P. A. G.; Sherrington, D. C. Facile synthesis of branched poly(methyl methacrylate)s. *J. Mater. Chem.* **2003**, *13*, 2701–2710.

(26) Henkel, R.; Vana, P. The Influence of RAFT on the Microstructure and the Mechanical Properties of Photopolymerized Poly (butyl acrylate) Networks. *Macromolecular Chemistry and Physics* **2014**, *215*, 182–189.

(27) Isaure, F.; Cormack, P. a. G.; Graham, S.; Sherrington, D. C.; Armes, S. P.; Bütün, V. Synthesis of branched poly(methyl methacrylate)s via controlled/living polymerisations exploiting ethylene glycol dimethacrylate as branching agent. *Chemical communications* **2004**, 1138–1139.

(28) Wang, A. R.; Zhu, S. Branching and gelation in atom transfer radical polymerization of methyl methacrylate and ethylene glycol dimethacrylate. *Polymer Engineering and Science* **2005**, *45*, 720–727.

(29) Tripathi, A. K.; Neenan, M. L.; Sundberg, D. C.; Tsavalas, J. G. Influence of n-alkyl ester groups on efficiency of crosslinking for methacrylate monomers copolymerized with EGDMA: Experiments and Monte Carlo simulations of reaction kinetics and sol-gel structure. *Polymer* **2016**, *96*, 130–145.

(30) Vo, C. D.; Rosselgong, J.; Armes, S. P.; Billingham, N. C. RAFT synthesis of branched acrylic copolymers. *Macromolecules* **2007**, *40*, 7119–7125.

(31) Yu, Q.; Zhang, J.; Cheng, M.; Zhu, S. Kinetic Behavior of Atom Transfer Radical Polymerization of Dimethacrylates. *Macromolecular Chemistry and Physics* **2006**, *207*, 287–294.

(32) Yu, Q.; Zhu, Y.; Ding, Y.; Zhu, S. Reaction Behavior and Network Development in RAFT Radical Polymerization of Dimethacrylates. *Macromolecular Chemistry and Physics* **2008**, *209*, 551–556.

(33) Mori, H.; Tsukamoto, M. RAFT polymerization of diacrylate derivatives having different spacers in dilute conditions. *Polymer* **2011**, *52*, 635–645.

(34) Gao, C.; Yan, D. Hyperbranched polymers: From synthesis to applications. *Progress in Polymer Science (Oxford)* **2004**, *29*, 183–275.

(35) Yan, M.; Lin, F.-Y.; Cochran, E. W. Dynamics of hyperbranched polymers derived from acrylated epoxidized soybean oil. *Polymer* **2017**, *125*, 117–125.

(36) Hernández, N.,; Yan, M.,; Williams, R.C.,; Cochran, E.W., *Green Polymer Chemistry: Biobased Materials and Biocatalysis*; ACS Symposium Series 1192; American Chemical Society, 2015; Vol. 1192; pp 183–199.

(37) Hassan, P. A.; Rana, S.; Verma, G. Making sense of Brownian motion: Colloid characterization by dynamic light scattering. *Langmuir* **2015**, *31*, 3–12.

(38) Moritz, H. U. Increase in viscosity and its influence on polymerization processes. *Chemical Engineering & Technology* **1989**, *12*, 71–87.

(39) Bannister, I.; Billingham, N. C.; Armes, S. P.; Rannard, S. P.; Findlay, P. Development of branching in living radical copolymerization of vinyl and divinyl monomers. *Macromolecules* **2006**, *39*, 7483–7492.

(40) Li, W.-H.; Hamielec, A. E.; Crowe, C. M. Kinetics of the free-radical copolymerization

of methyl methacrylate/ethylene glycol dimethacrylate: 1. Experimental investigation. *Polymer* **1989**, *30*, 1513–1517.

(41) Klein, D. J. Rigorous results for branched polymer models with excluded volume. *The Journal of Chemical Physics* **1981**, *75*, 5186.

(42) Schmidt, R.; Hernández Cifre, J.; de la Torre, J. Multi-Scale Simulation of Hyperbranched Polymers. *Polymers* **2015**, *7*, 610–628.

(43) Burchard, W. Solution Properties of Branched Macromolecules. *Advances in Polymer Science* **1999**, *143*, 113–194.

(44) Del Río Echenique, G.; Schmidt, R. R. R.; Freire, J. J.; Hernández Cifre, J. G.; García De La Torre, J. A multiscale scheme for the simulation of conformational and solution properties of different dendrimer molecules. *Journal of the American Chemical Society* **2009**, *131*, 8548–8556.

(45) Karatasos, K.; Adolf, D. B.; Davies, G. R. Statics and dynamics of model dendrimers as studied by molecular dynamics simulations. *The Journal of Chemical Physics* **2001**, *115*, 5310.

(46) Gao, H.; Min, K.; Matyjaszewski, K. Determination of gel point during atom transfer radical copolymerization with cross-linker. *Macromolecules* **2007**, *40*, 7763–7770.

(47) Li, W.; Gao, H.; Matyjaszewski, K. Influence of initiation efficiency and polydispersity of primary chains on gelation during atom transfer radical copolymerization of monomer and cross-linker. *Macromolecules* **2009**, *42*, 927–932.

(48) Rieger, J.; Stoffelbach, F.; Bui, C.; Alaimo, D.; Jérôme, C.; Charleux, B. Amphiphilic poly(ethylene oxide) macromolecular RAFT agent as a stabilizer and control agent in ab initio batch emulsion polymerization. *Macromolecules* **2008**, *41*, 4065–4068.

(49) Koh, M. L.; Konkolewicz, D.; Perrier, S. S. A simple route to functional highly branched structures: RAFT homopolymerization of divinylbenzene. *Macromolecules* **2011**, *44*, 2715–2724.

(50) Lin, Y.; Liu, X.; Li, X.; Zhan, J.; Li, Y. Reversible Addition-Fragmentation Chain Transfer Mediated Radical Polymerization of Asymmetrical Divinyl Monomers Targeting Hyperbranched Vinyl Polymers. *Journal of Polymer Science Part A: Polymer Chemistry* **2007**, *45*, 26–40.

(51) Skey, J.; O'reilly, R. K. Synthesis of chiral micelles and nanoparticles from amino acid based monomers using RAFT polymerization. *Journal of Polymer Science Part A: Polymer Chemistry* **2008**, *46*, 3690–3702.

(52) Bergman, J. A.; Hernández, N. B.; Cochran, E. W.; Heinen, J. M. Thermodynamics of chain architecture in acrylic block terpolymers. *Macromolecules* **2014**, *47*, 5960–5970.

(53) Jiang, C.; Shen, Y.; Zhu, S.; Hunkeler, D. Gel formation in atom transfer radical polymerization of 2-(N,N-dimethylamino)ethyl methacrylate and ethylene glycol dimethacrylate. *Journal of Polymer Science Part A: Polymer Chemistry* **2001**, *39*, 3780–3788.

(54) Gao, H.; Li, W.; Matyjaszewski, K. Synthesis of polyacrylate networks by ATRP: Parameters influencing experimental gel points. *Macromolecules* **2008**, *41*, 2335–2340.

(55) Gao, H.; Polanowski, P.; Matyjaszewski, K. Gelation in living copolymerization of monomer and divinyl cross-linker: Comparison of ATRP experiments with Monte Carlo simulations. *Macromolecules* **2009**, *42*, 5925–5932.

(56) Van Camp, W.; Gao, H.; Prez, F. E.; Matyjaszewski, K. Effect of crosslinker multiplicity on the gel point in ATRP. *Journal of Polymer Science, Part A: Polymer Chemistry* **2010**, *48*, 2016–2023.

(57) Rosselgong, J.; Armes, S. P.; Barton, W. R. S.; Price, D. Synthesis of branched methacrylic Copolymers: Comparison between RAFT and ATRP and effect of varying the monomer concentration. *Macromolecules* **2010**, *43*, 2145–2156.

For Table of Contents Use Only

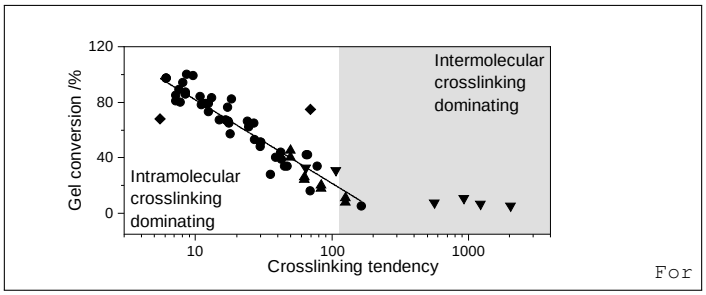

For